ADVANCING EARTH AND SPACE SCIENCE

Geophysical Research Letters

RESEARCH LETTER
10.1029/2020GL088395

Key Points:
- The frontal part of Japan Trench plate boundary fault, which slipped during the 2011 Tohoku-Oki earthquake, is composed of 80% smectite
- Our experiments indicate that this material behaves like a fluid during faulting, whereby the shear stress is governed mostly by cohesion
- Cohesional slip, rather than frictional slip, may be a realistic faulting process in this fault zone

Supporting Information:
- Supporting Information S1

Correspondence to:
J. Kameda,
kameda@sci.hokudai.ac.jp

Citation:
Kameda, J., & Hamada, Y. (2020). Cohesional slip on a plate subduction boundary during a large earthquake. *Geophysical Research Letters*, *47*, e2020GL088395. https://doi.org/10.1029/2020GL088395

Received 13 APR 2020
Accepted 31 AUG 2020
Accepted article online 9 SEP 2020

Cohesional Slip on a Plate Subduction Boundary During a Large Earthquake

Jun Kameda[1] and Yohei Hamada[2]

[1]Department of Earth and Planetary Sciences, Graduate School of Science, Hokkaido University, Sapporo, Japan, [2]Kochi Institute for Core Sample Research, X-star, Japan Agency for Marine-Earth Science and Technology (JAMSTEC), Nankoku, Japan

Abstract The frontal part of the Japan Trench plate boundary fault, which slipped during the 2011 Tohoku-Oki earthquake (M_w 9.0), is enriched in smectite and is intrinsically weak owing to the high swelling pressure of this mineral. Our rheometric experiments using analog fault materials demonstrate that "cohesional slip," rather than frictional slip, is a realistic faulting process in the studied fault zone. The cohesional slip can be described by the Bingham plastic model. Consequently, the coseismic shear stress is described by the yield stress and plastic viscosity. Comparison of the results with the average shear stress derived from a previous study suggests that the slip zone thickness for cohesional slip is ~1.3 cm or less. This finding is consistent with textures characterized by discrete slip planes of comparable thickness observed in the recovered fault rocks, suggesting that these slip planes were activated during the Tohoku-Oki earthquake.

Plain Language Summary Fault behavior is commonly understood to be governed by rock frictional properties. However, this does not hold for fault zones rich in sticky clay minerals. One such example is the frontal part of the Japan Trench plate boundary fault, which slipped during the 2011 Tohoku-Oki earthquake (M_w 9.0) and is composed of 80% smectite (a clay mineral). Our experiments indicate that this fault material can behave like a fluid during faulting. The present results, together with previous findings, suggest that faulting process in the studied fault zone is governed mostly by cohesional properties of the fault material rather than frictional.

1. Introduction

The rupture and slip of the 2011 Tohoku-Oki earthquake (M_w 9.0) caused ~50 m of coseismic displacement near the seafloor (Fujii et al., 2011; Fujiwara et al., 2011; Ide et al., 2011; Kodaira et al., 2012) and generated a huge tsunami that struck the northeastern coast of Honshu, Japan. To investigate the faulting process of the earthquake, a deep-sea drilling survey (Japan Trench Fast Drilling Project Expedition 343 and 343T program; JFAST) was undertaken by the Integrated Ocean Drilling Program (IODP) at a site located ~7 km landward of the Japan Trench in the region where the largest displacement was observed (Chester et al., 2012, 2013). The survey identified a plate boundary fault zone containing 60–80 wt.% smectite within pelagic clay strata (Kameda et al., 2015). Such a smectite-rich material has very low shear strength, as demonstrated by laboratory shear experiments at seismic to subseismic slip rates (Ikari et al., 2007, 2015; Remitti et al., 2015; Saffer & Marone, 2003; Ujiie et al., 2013), and this property likely facilitated coseismic movement of the shallow portion of the plate boundary fault. The weakness of the fault has also been inferred from borehole temperature observations, which detected shear heating during the earthquake (Fulton et al., 2013). On the basis of the temperature anomaly at the plate boundary, the energy dissipated during the coseismic slip is estimated to have been 27 MJ/m^2, equivalent to an apparent frictional coefficient of 0.08 (Fulton et al., 2013).

Recently, we found that the smectite-rich plate boundary fault zone material has high swelling ability, with the in situ swelling pressure being almost equivalent to the effective normal stress applied on the fault (Kameda et al., 2019). Should this equilibrium state be achieved, the modified Mohr-Coulomb failure criterion (Chatterji & Morgenstern, 1990) implies that the shear strength of the fault can be attributed mainly to cohesion. The behavior of fault movement is commonly understood to be governed by rock frictional properties (Scholz, 2002). However, this does not hold for cohesive samples that include clay minerals (Ikari & Kopf, 2011, 2015). Ikari et al. (2015) measured the cohesional strength of Tohoku fault

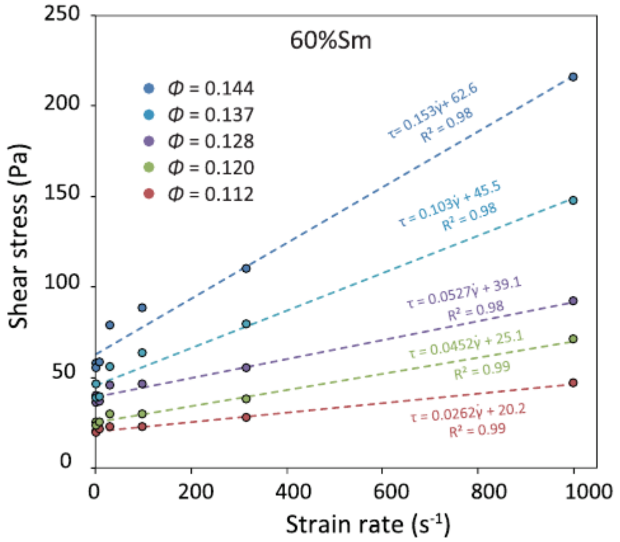

Figure 1. Flow curves (shear stress vs. strain rate) for samples of a solid mixture of 60 wt.% smectite and 40 wt.% quartz (60%Sm) as a function of the solid fraction ϕ.

zone samples by using a direct shear apparatus and reported a cohesional strength of less than ~300 kPa but did not document the dependence of slip rate on cohesional strength. As sediment-water composites or smectite-rich bentonite suspensions commonly exhibit viscoplastic behavior (e.g., Brandenburg & Lagaly, 1988; Kelessidis, 2017; Torrance & Pirnat, 1984; Torrance, 1999; Tomba'cz & Szekeres, 2004), cohesional strength can be a function of shear rate.

During this study, we conducted rheometric experiments using smectite-quartz mixtures as analogs of natural Tohoku fault material to investigate the behavior of "cohesional slip," whereby a fault is displaced with a shear stress generated only from the cohesional force of the fault zone material. Rheological properties of similar materials have been examined by Kameda and Morisaki (2017), but here we additionally investigate the dependence of these properties on sample porosity, which enables us to extrapolate the data to the in situ conditions of the fault zone. Using the new results, as well as observations of textures of natural fault rocks, we investigate the occurrence of this mode of slip during the 2011 Tohoku-Oki earthquake.

2. Methods

2.1. Materials and Sample Preparation

Experimental samples were prepared by mixing high-purity Na-smectite (Kunipia-F; Kunimine Industries) and crystalline quartz (silicon dioxide 199-00625; Wako Pure Chemical Industries). As the smectite content in the natural fault samples varies from 57 to 84 wt.% with a mean of 71 wt.% (Kameda et al., 2015), we tested samples with smectite weight fractions of 60, 70, and 80 wt.% (hereafter termed 60%Sm, 70%Sm, and 80%Sm, respectively). Detailed information on the standard samples is given by Kameda and Morisaki (2017). The solid mixtures were dispersed in NaCl solutions (0.6 *M*) because the pore fluid of the natural fault rock has high ionic strength comparable with that of seawater (Kameda et al., 2016). A 50-ml polypropylene conical tube was used to prepare the suspensions with different water contents. The tubes were shaken for at least 1 hr using a laboratory mixer to homogenize the samples before the experiments.

2.2. Rheological Measurements

All of the rheological tests were conducted using an HR-2 rheometer (TA Instruments) with a parallel plate geometry. This rheometer comprises a 40-mm-diameter aluminum rotational upper plate and a stationary lower Peltier plate, with the latter being a thermoelectric plate that allows the temperature to be controlled (at 20°C during this study). To avoid the influence of wall slip (i.e., slip between the sample and the adjacent metal plate, rather than within the sample), which is a common problem in rheometric experiments (Coussot & Piau, 1994), 100 grit ($\varphi = 125$ μm) waterproof sandpaper was attached to the conventional flat plate. Samples were loaded into a 1-mm gap between the upper and lower plates by using a spatula. Before each test, samples were presheared at a strain rate $\dot{\gamma}$ of 50 s^{-1} for 20 s to release the initial anomalous stress (Heymann et al., 2002) and then rested for 3 min. Rheological properties were tested by measuring shear stress τ under the applied $\dot{\gamma}$ (with torque being recorded every 5 s), which was increased in a stepwise manner from 1 to 1,000 s^{-1} (nominally seven steps: 1, 3.2, 10, 32, 100, 320, and 1,000 s^{-1}). At each step, the shear stress value was acquired after the torque change in three successive sample periods (i.e., after 15 s) was within 3% or after the total period exceeded 45 s (we set the maximum recording period of 45 s based on the expected duration of 50 s for earthquake slip; Fulton et al., 2013).

3. Experimental Results

Figure 1 shows a series of flow curves (shear stress vs. strain rate) for the 60%Sm samples at different water contents (flow curves for 70%Sm and 80%Sm are presented in Figure S1 in the supporting information). In this plot, water content was recalculated to the solid volumetric fraction ϕ following the procedure given

10.1029/2020GL088395

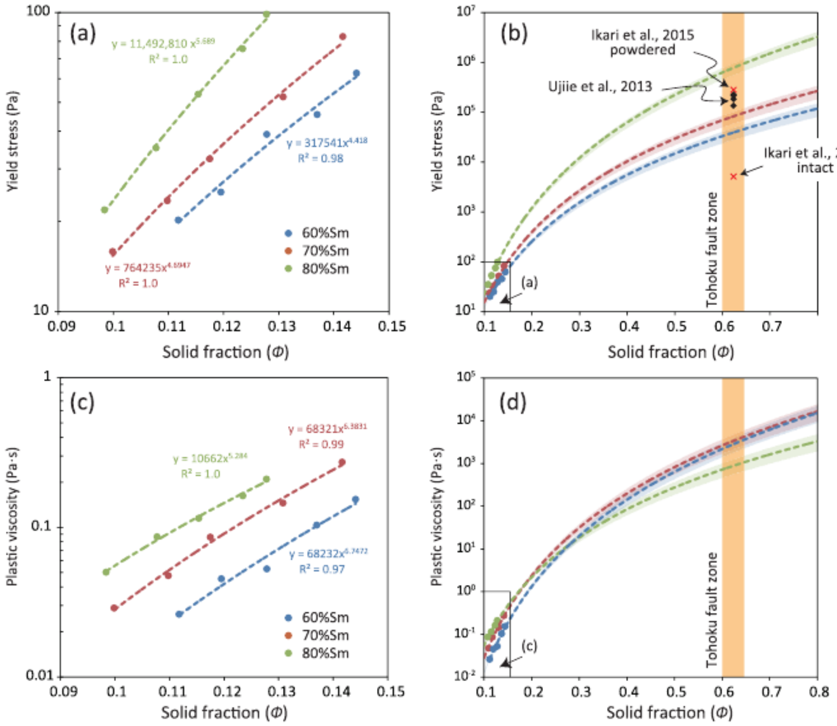

Figure 2. (a and c) Summary plots of yield stress and plastic viscosity versus solid fraction. (b and d) Extrapolation of the fitted curves in (a) and (c). Yield stress and plastic viscosity are shown by the extrapolated curves; shaded areas show the corresponding error. The porosity of the Tohoku fault zone is shown by the vertical orange bar ($\phi = 0.60$–0.64). The cohesional strength from direct measurements (Ikari et al., 2015) and the shear stress at zero normal load from high-velocity shear experiments (Ujiie et al., 2013) are also shown in (b).

in the supporting information. Although the data are scattered in the low-strain-rate region (<30 s^{-1}), the flow curves overall show an almost linear correlation between stress and strain rate $\dot{\gamma}$, which can be reasonably fitted by the following equation for a Bingham fluid with fitting degrees of >0.95:

$$\tau = \tau_B + \eta\dot{\gamma}, \tag{1}$$

whereτ is the shear stress, τ_B is the Bingham yield stress, and η is the plastic viscosity.

Figures 2a and 2c show variations in the Bingham yield stress and the plastic viscosity of the samples as a function of the solid fraction, respectively (rheological parameters determined from the experiments are summarized in Table S1). In general, the Bingham yield stress of bentonite suspensions exhibits a power law dependence on the solid fraction (Kelessidis, 2017; Ramos-Tejada et al., 2001):

$$\tau_B = a(\phi)^b, \tag{2}$$

where a and b are fitting parameters. As shown in Figures 2a and 2c, the plastic viscosity, along with the yield stress, can be expressed by this power law function. Repeated measurements revealed that the uncertainties in the rheological parameters were within ±5%.

On the basis of resistivity logging data from the JFAST borehole, the porosity of the fault zone is estimated to vary from 36% to 40% (Kameda et al., 2019), corresponding to a solid fraction of 0.60–0.64. Thus, extrapolation of Equation 2 to the fault zone condition provides estimates of yield stress and plastic viscosity that range from 30 to 900 kPa (potential error of ±30%) and 0.7 to 3.3 kPa·s (potential error of ±40%), respectively (Figures 2b and 2d), depending on the smectite content of the solid mixture (the error on the yield stress and plastic viscosity is shown by the shaded area for each extrapolated curve).

10.1029/2020GL088395

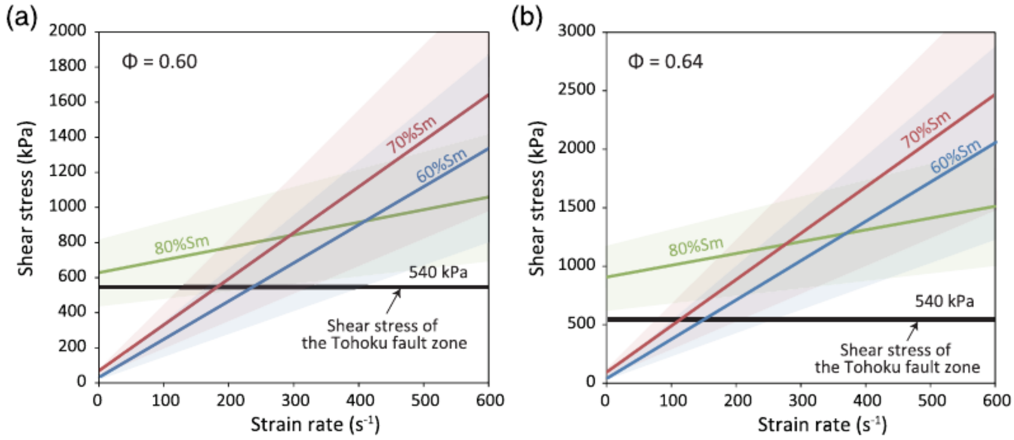

Figure 3. (a and b) Correlation between shear stress and strain rate for the cohesional slip behavior of the Tohoku fault zone at the boundary conditions of the solid fraction: (a) $\phi = 0.60$ and (b) $\phi = 0.64$. The error on the shear stress for each solid line is shown by the shaded area. The black lines in (a) and (b) represent the average coseismic shear stress of the fault estimated from temperatures measured in the JFAST borehole (540 kPa; Fulton et al., 2013).

4. Discussion

The present rheometric experiments indicate that the analyzed samples behave as Bingham fluids. However, the solid fractions for these data are much smaller than those in natural fault zones. During this study, the range of values for the solid fraction was limited because of the torque limitation of the rheometric device. In addition, samples with higher solid fractions caused slip between the sample and the lower Peltier plate, making precise measurements difficult under such conditions. Although the correlation between yield stress and solid fraction found in this study has been recognized for a variety of materials and values of solid fraction (up to ~0.6; Jeong, 2019; Zhou et al., 1999), its validity for smectitic samples should be verified by conducting experiments using appropriate apparatuses and experimental conditions in the future. Nevertheless, the extrapolated yield stress values of the Tohoku fault zone (20–1,200 kPa) are not so different from the cohesional strength values of the JFAST samples measured by previous studies (Ikari et al., 2015; Ujiie et al., 2013; Figure 2).

Ikari et al. (2015) found that the cohesional strength of intact samples (~5 kPa) is lower than that of powdered samples (270 kPa) and suggested that this might be due to the elimination of strong water-clay bonding on foliation surfaces in the intact samples. As intact samples have deformation textures that result in heterogeneity in mineral composition or porosity, we infer that along with the above possibility involving water-clay bonding, such heterogeneity can cause a difference in cohesional strength between intact and powdered samples. The high-velocity shear experiments of Ujiie et al. (2013) demonstrated a dependence of shear stress on normal load. From this correlation, the shear stress at zero normal load is estimated to be 130–220 kPa (Figure 1c in Ujiie et al., 2013). Although those experimental data cannot be readily compared with ours, as the previous test was conducted using distilled water and water chemistry can modify the rheological properties of smectite-containing samples (Kelessidis, 2017), the stress values are comparable with the yield stress obtained in the present study (Figure 2b). In addition, the shear stress experiments of Ujiie et al. (2013) were conducted under a particular range of strain rates, with the values obtained therefore representing the upper bounds of yield stress. Thus, the yield stresses for the 60%Sm and 70%Sm samples of the present study represent plausible values for in situ conditions.

Figures 3a and 3b show the possible behavior of the studied fault zone materials at the upper and lower bounds of the solid fraction (0.64 and 0.60, respectively). The error for each solid line is shown by the shaded area. We term this faulting process "cohesional slip," as the shear stress during the slip is generated under zero normal load and can thus be attributed solely to the cohesion of the material. Figure 3 also shows the average shear stress constrained from temperature observations in the JFAST borehole (540 kPa; Fulton et al., 2013). As noted, the 80%Sm sample exhibits somewhat higher yield stress than the other

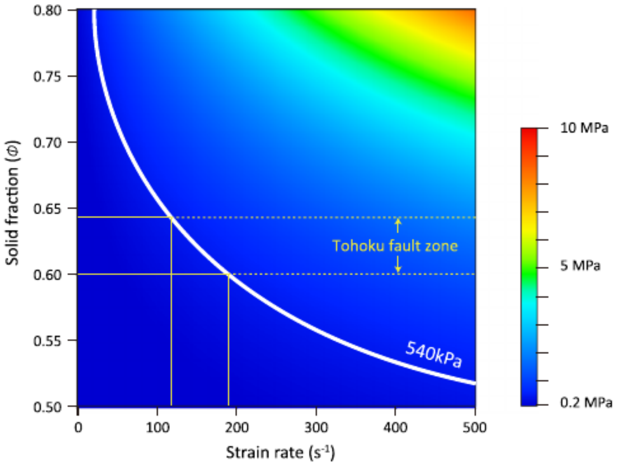

Figure 4. Correlation between solid fraction, strain rate and shear stress for the 70%Sm sample. Yield stress and plastic viscosity were calculated from the fitted lines in Figures 2a and 2c. The white curve represents the average coseismic shear stress of the fault (540 kPa; Fulton et al., 2013), estimated from temperatures measured in the JFAST borehole.

samples. Under natural conditions, fault displacement would be preferentially accommodated along weaker horizons when rupture and slip propagate from depth. Therefore, the lines for the 60%Sm and 70%Sm samples are more likely to describe the slip zone properties of the earthquake compared with the 80%Sm line. A comparison of the present results with the shear stress study of Fulton et al. (2013) suggests that the strain rate ranges from ~130 to ~430 s^{-1} at $\phi = 0.60$ and from ~80 to ~280 s^{-1} at $\phi = 0.64$.

Figure 4 shows details of the correlation between the solid fraction, strain rate, and shear stress for the 70%Sm sample, along with the coseismic shear stress of the Tohoku fault zone (540 kPa). This plot similarly indicates that the expected strain rate is highly dependent on the solid fraction, and the borehole porosity data suggest that the strain rate ranged from ~120 to ~190 s^{-1} during the Tohoku-Oki earthquake.

The shear stress depicted in Figure 4 was estimated under the assumption that the slip zone temperature is constant during slip. In reality, the temperature would increase to some extent owing to shear heating after the onset of slip. In the case of a 1-cm-thick slip zone, coseismic slip results in a maximum temperature of ~800°C, with the temperature being lower in cases where the slip zone is wider (Fulton et al., 2013). According to Vryzas et al. (2017), the flow behavior of a bentonite suspension is temperature dependent; that is, with increasing temperature, yield stress increases because of a stronger association between individual smectite particles, whereas viscosity decreases mainly because of a decrease in dispersant water viscosity. The yield stress likely represents the in situ fault zone condition, as the background (i.e., preslip) temperature (~25°C; Fulton et al., 2013) is very similar to the experimental temperature. Conversely, plastic viscosity may decrease owing to temperature increase in the slip zone, suggesting that the strain rate increases successively during coseismic slip.

The actual slip zone thickness for the Tohoku-Oki earthquake is poorly defined. Core observations have revealed that deformation textures of the fault zone are characterized by pervasive scaly fabrics that are crosscut by multiple discrete slip planes with thicknesses of ~1 cm or less (Kirkpatrick et al., 2015). These slip planes might have formed as a result of coseismic slip, such as that of the Tohoku-Oki earthquake, whereas the pervasive scaly fabrics might represent deformation at low strain rates (Kirkpatrick et al., 2015). In contrast, on the basis of the structural properties of constituent smectite in the fault zone, Schleicher et al. (2015) argued for the likelihood of a slip zone much wider than ~1 cm. As noted, the strain rate during the Tohoku-Oki earthquake might have exceeded ~80 s^{-1}, implying that the slip zone thickness is ~1.3 cm or less for a slip rate in the order of 1 m/s (Fulton et al., 2013). This value is consistent with textural observations of natural fault samples (Kirkpatrick et al., 2015). It is uncertain why the coseismic deformation is localized in such a thin slip zone. As mentioned above, our experiments suggest that the rheological properties of the fault zone can be highly sensitive to smectite content, and even a small perturbation in smectite content in the original deposits could enhance the localization of shear. Pelagic clays, which could be stratigraphically equivalent to the fault zone (Kirkpatrick et al., 2015), contain millimeter-scale laminations, and this could be one reason for the localized production of a thin, slippery plane during the Tohoku-Oki earthquake.

5. Conclusions

We examined the rheological properties of smectite-quartz suspensions to clarify the coseismic slip behavior of the Tohoku-Oki fault zone. We show that the materials behave as a Bingham fluid, with rheological parameters being dependent on the solid fraction and smectite content. The former dependency was utilized to constrain the magnitude of shear stress of the suspensions equivalent to the in situ fault zone conditions. The range of reproduced slips can simultaneously explain previous findings of coseismic shear stress constrained from heating signatures at the borehole as well as rock deformation textures with a realistic value of smectite content. This result, as well as the findings of a previous experiment on fault rock swelling, indicates that "cohesional slip," whereby the shear stress during fault slip is governed mostly by rock cohesion, is a likely behavior of the studied fault zone during an earthquake. This work also underlines the importance of the precise evaluation of cohesion in understanding fault mechanics.

Data Availability Statement

The experimental raw data are available at Zenodo (http://doi.org/10.5281/zenodo.3976387).

Acknowledgments

We thank two anonymous reviewers and Editor Jeroen Ritsema for their constructive comments, which greatly improved the manuscript. This work was supported by a Grant-in-Aid for Scientific Research (18H0129508) from the Japan Society for the Promotion of Science.

References

Brandenburg, U., & Lagaly, G. (1988). Rheological properties of sodium montmorillonite dispersions. *Applied Clay Science*, *3*(3), 263–279. https://doi.org/10.1016/0169-1317(88)90033-6

Chatterji, P. K., & Morgenstern, N. R. (1990). A modified shear strength formulation for swelling of clay soils. In K. B. Hoddinott, & R. O. Lamb (Eds.), *Physico-chemical aspects of soil and related materials*, *ASTMSTP* (Vol. 1095, pp. 118–135). Philadelphia: ASTM International. https://doi.org/10.1520/STP23552S

Chester, F. M., Mori, J. J., Toczko, S., Eguchi, N. & the Expedition 343/343T Scientists, (2012). Japan Trench Fast Drilling Project (JFAST). IODP Preliminary Report 343/343T. https://10.2204/iodp.pr.343343T

Chester, F. M., Rowe, C., Ujiie, K., Kirkpatrick, J., Regalla, C., Remitti, F., et al. (2013). Structure and composition of the plate-boundary slip zone for the2011 Tohoku-Oki earthquake. *Science*, *342*(6163), 1208–1211. https://doi.org/10.1126/science.1243719

Coussot, P., & Piau, J. M. (1994). On the behavior of fine mud suspensions. *Rheologica Acta*, *33*, 175–184.

Fujii, Y., Satake, K., Sakai, S., Shinohara, M., & Kanazawa, T. (2011). Tsunami source of the 2011 off the Pacific coast of Tohoku earthquake. *Earth, Planets and Space*, *63*(7), 815–820. https://doi.org/10.5047/eps.2011.06.010

Fujiwara, T., Kodaira, S., No, T., Kaiho, Y., Takahashi, N., & Kaneda, Y. (2011). The 2011 Tohoku-oki earthquake: Displacement reaching the trench axis. *Science*, *334*(6060), 1240. https://doi.org/10.1126/science.1211554

Fulton, P. M., Brodsky, E. E., Kano, Y., Mori, J., Chester, F. M., Ishikawa, T., et al. (2013). Low coseismic friction on the Tohoku-oki fault determined from temperature measurements. *Science*, *342*(6163), 1214–1217. https://doi.org/10.1126/science.1243641

Heymann, L., Peukert, S., & Aksel, N. (2002). Investigation of the solid-liquid transition of highly concentrated suspensions in oscillatory amplitude sweeps. *Journal of Rheology*, *46*(1), 93–112. https://doi.org/10.1122/1.1423314

Ide, S., Baltay, A., & Beroza, G. C. (2011). Shallow dynamic overshoot and energetic deep rupture in the 2011 *Mw* 9.0 Tohoku-oki earthquake. *Science*, *332*(6036), 1426–1429. https://doi.org/10.1126/science.1207020

Ikari, M. J., Kameda, J., Saffer, D. M., & Kopf, A. J. (2015). Strength characteristics of Japan Trench borehole samples in the high-slip region of the 2011 Tohoku-Oki earthquake. *Earth and Planetary Science Letters*, *412*, 35–41.

Ikari, M. J., & Kopf, A. J. (2011). Cohesive strength of clay-rich sediment. *Geophysical Research Letters*, *38*, L16309. https://doi.org/10.1029/2011GL047918

Ikari, M. J., & Kopf, A. J. (2015). The role of cohesion and overconsolidation in submarine slope failure. *Marine Geology*, *369*, 153–161. https://doi.org/10.1016/j.margeo.2015.08.012

Ikari, M. J., Saffer, D. M., & Marone, C. (2007). Effect of hydration state on the frictional properties of montmorillonite-based fault gouge. *Journal of Geophysical Research*, *112*, B06423. https://doi.org/10.1029/2006JB004748

Jeong, S. W. (2019). Shear rate-dependent rheological properties of mine tailings: Determination of dynamic and static yield stresses. *Applied Sciences*, *9*(22), 4744. https://doi.org/10.3390/app9224744

Kameda, J., Inaoi, C., & Conin, M. (2016). Exchangeable cation composition of the smectite-rich plate boundary fault at the Japan Trench. *Geophysical Research Letters*, *43*, 3112–3119. https://doi.org/10.1002/2016GL068283

Kameda, J., & Morisaki, T. (2017). Sensitivity of clay suspension rheological properties to pH, temperature, salinity and smectite-quartz ratio. *Geophysical Research Letters*, *44*, 9615–9621. https://doi.org/10.1002/2017GL075334

Kameda, J., Shimizu, M., Ujiie, K., Hirose, T., Ikari, M., Mori, J., et al. (2015). Pelagic smectite as an important factor in tsunamigenic slip along the Japan Trench. *Geology*, *43*(2), 155–158. https://doi.org/10.1130/G35948.1

Kameda, J., Uno, M., Conin, M., Ujiie, K., Hamada, Y., & Kimura, G. (2019). Fault weakening caused by smectite swelling. *Earth, Planets and Space*, *71*, 131. https://doi.org/10.1186/s40623-019-1108-5

Kelessidis, V. (2017). Yield stress of bentonite dispersions. *Rheology*, *1*, 101.

Kirkpatrick, J. D., Rowe, C. D., Ujiie, K., Moore, J. C., Regalla, C., Remitti, F., et al. (2015). Structure and lithology of the Japan Trench subduction plate boundary fault. *Tectonics*, *34*, 53–69. https://doi.org/10.1002/2014TC003695

Kodaira, S., No, T., Nakamura, Y., Fujiwara, T., Kaiho, Y., Miura, S., et al. (2012). Coseismic fault rupture at the trench axis during the 2011 Tohoku-oki earthquake. *Nature Geoscience*, *5*(9), 646–650. https://doi.org/10.1038/NGEO1547

Ramos-Tejada, M. M., Arroyo, F. J., Perea, R., & Du'ran, J. D. G. (2001). Scaling behavior of the rheological properties of montmorillonite suspensions: Correlation between interparticle interaction and degree of flocculation. *Journal of Colloid and Interface Science*, *235*(2), 251–259. https://doi.org/10.1006/jcis.2000.7370

Remitti, F., Smith, S. A. F., Mittempergher, S., Gualtieri, A. F., & Di Toro, G. (2015). Frictional properties of fault zone gouges from the J-FAST drilling project (*Mw* 9.0 2011 Tohoku-Oki earthquake). *Geophysical Research Letters*, *42*, 2691–2699. https://doi.org/10.1002/2015GL063507

Saffer, D. M., & Marone, C. (2003). Comparison of smectite- and illite-rich gouge frictional properties: Application to the updip limit of the seismogenic zone along subduction megathrusts. *Earth and Planetary Science Letters*, *215*(1-2), 219–235. https://doi.org/10.1016/S0012-821X(03)00424-2

Schleicher, A. M., Boles, A., & van der Pluijm, B. A. (2015). Response of natural smectite to seismogenic heating and potential implications for the 2011 Tohoku earthquake in the Japan Trench. *Geology*, *43*(9), 755–758. https://doi.org/10.1130/G36846.1

Scholz, C. H. (2002). *The mechanics of earthquake and faulting* (p. 471). Cambridge: Cambridge University Press. https://doi.org/10.1017/CBO9780511818516

Tomba'cz, E., & Szekeres, M. (2004). Colloidal behavior of aqueous montmorillonite suspensions: The specific role of pH in the presence of indifferent electrolytes. *Applied Clay Science*, *27*(1-2), 75–94. https://doi.org/10.1016/j.clay.2004.01.001

Torrance, J. K. (1999). Physical, chemical and mineralogical influences on the rheology of remoulded low-activity sensitive marine clay. *Applied Clay Science*, *14*(4), 199–223. https://doi.org/10.1016/S0169-1317(98)00057-X

Torrance, J. K., & Pirnat, M. (1984). Effect of pH on the rheology of marine clay from the site of the south nation river, Canada, landslide of 1971. *Clays and Clay Minerals*, *32*(5), 384–390. https://doi.org/10.1346/CCMN.1984.0320506
Ujiie, K., Tanaka, H., Saito, T., Tsutsumi, A., Mori, J. J., Kameda, J., et al. (2013). Low coseismic shear stress on the Tohoku-Oki megathrust determined from laboratory experiments. *Science*, *342*(6163), 1211–1214. https://doi.org/10.1126/science.1243485
Vryzas, Z., Kelessidis, V. C., Nalbantian, L., Zaspalis, V., & Gerogiorgis, D. I. (2017). Effect of temperature on the rheological properties of neat aqueous Wyoming sodium bentonite dispersions. *Applied Clay Science*, *136*, 26–36.
Zhou, Z., Solomon, M. J., Scales, P. J., & Boger, D. V. (1999). The yield stress of concentrated flocculated suspensions of size distributed particles. *Journal of Rheology*, *43*(3), 651–671. https://doi.org/10.1122/1.551029

References From the Supporting Information

Deer, W. A., Howie, R. A., & Zussman, J. (1992). *An introduction to the rock-forming minerals* (p. 696). Hong Kong: Longman Group Limited.
Keren, R., & Shainberg, I. (1975). Water vapor isotherms and heat of immersion of Na/Ca montmorillonite systems—I: Homoionic clay. *Clays and Clay Minerals*, *23*(3), 193–200. https://doi.org/10.1346/CCMN.1975.0230305
Miyawaki, R., Sano, T., Ohashi, F., Suzuki, M., Kogure, T., Okumura, T., et al. (2010). Some reference data for the JCSS clay specimens (technical report), Nendo-Kagaku, 4, 158–198.
Tachi, Y., & Yotsuji, K. (2014). Diffusion and sorption of Cs^{+}, Na^{+}, I^{-} and HTO in compacted sodium montmorillonite as a function of pore water salinity: Integrated sorption and diffusion model. *Geochimica et Cosmochimica Acta*, *132*, 75–93. https://doi.org/10.1016/j.gca.2014.02.004